Reflectionless Tilted Grating Couplers With Improved Coupling Efficiency Based on a Silicon Overlay

Yanlu Li, Lianyan Li, Bin Tian, Gunther Roelkens, and Roel G. Baets, *Fellow, IEEE*

Abstract—Grating couplers are important photonic devices on a complementary metal-oxide-semiconductor compatible silicon-on-insulator platform to couple light between optical waveguides and free space optical components or fibers. In this letter, we report the combination of a tilted grating coupler design, which strongly suppresses the back-reflection for light incident on the grating coupler from a waveguide, and a silicon overlay locally deposited on top of the grating region, which enhances the coupling efficiency of the grating coupler, by means of simulation and experiment. The fabricated tilted focusing grating couplers with silicon overlay show a coupling efficiency of −2.2 dB in combination with a back-reflection of around −40 dB when excited from the silicon waveguide. The tilted design also provides an alternative approach to enhance the transmission of a grating coupler when the thickness of the Si overlay is not optimized.

Index Terms—Tilted grating coupler, back-reflection, coupling efficiency.

I. Introduction

GRATING couplers (GCs) are used in photonic integrated circuits (PICs) to couple light between optical waveguides and free space optical components or fibers [1]. They provide a simple method for wafer scale testing of PICs, which can help to reduce the cost of production. For a specific GC design, both its back-reflection and its coupling efficiency (to free space or to a single-mode fiber) should be optimized over the required spectral band. On one hand it is important to reduce the back-reflection for light incident on the GC from the waveguide. The back-reflection of a commonly used one-dimensional (1D) GC comes from two major sources: the second order reflection of the GC and the Fresnel reflection on the boundary between the input waveguide and the GC. The second order reflection is usually suppressed by setting the zenith angle of the output light ϕ_0 (the angle of the output light with respect to the chip normal) to a non-zero value (e.g. 10°) [2]. By improving
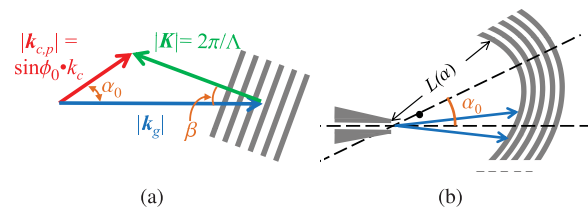
Fig. 1. (a) Wave vector relations in a tilted 1D grating coupler; (b) a tilted focusing grating coupler.

the mode matching conditions or using an apodized grating design, the Fresnel back-reflection can also be reduced [4]–[7]. However, these techniques may not be sufficient to reduce the reflections to an adequate level. Alternatively the back-reflection can be strongly reduced by directing the reflection away from the input waveguide by means of a tilted grating coupler [3]. On the other hand, studies on improving the coupling efficiency and bandwidth of a GC have also been intensively reported [2], [8]. We reported that a silicon overlay can be deposited on top of a 1D GC to increase the coupling efficiency [9], [10]. However, there has been little work so far on designs that combine high coupling efficiency with low back reflection in a CMOS-compatible SOI platform. In this letter, we report about the coupling efficiency of different tilted 1D GC and tilted focusing grating coupler (FGC) designs with Si overlays, by means of simulation and measurement. We demonstrate for the first time that the combination of tilting and overlay does indeed lead to a very relevant performance improvement for fiber-chip coupling. This improvement is of key importance in all applications where spurious reflections matter. Unlike many other designs that are fabricated with the use of electron beam lithography, our designs are realized in an advanced CMOS-compatible platform and thus are suitable for high volume production.

II. Theory on Tilted Grating Couplers With Si Overlay

Two different tilted GC designs, the tilted 1D GC and the tilted FGC, can be used to suppress back reflections for light sent from the input waveguides to the GCs, because these reflections are not sent back directly to the input waveguides. For a tilted 1D GC, the relations among the wave vector of the input light ($\vec{k}_g$), the reciprocal lattice vector of the grating ($\vec{K}$), and the projection of the output light wave vector onto the chip surface ($\vec{k}_{c,p}$) are shown in figure 1(a). According to these relations, the tilt angle of the GC β and the grating period Λ are calculated according to the required direction of

the output light, being described by the zenith angle ϕ_0 and the azimuth α_0, with the following equations:

$$\beta(\phi_0, \alpha_0) = \arctan\left(\frac{n_{c,p} \sin\alpha_0}{n_g^0 - n_{c,p} \cos\alpha_0}\right), \qquad (1)$$

$$\Lambda(\phi_0, \alpha_0) = \frac{\lambda_0 \cos\beta(\phi_0, \alpha_0)}{n_g^0 - n_{c,p} \cos\alpha_0}, \qquad (2)$$

where $n_{c,p} = n_c \sin\phi_0$, λ_0 is the vacuum wavelength of the light, n_g^0 is the effective index of the light propagating in the waveguide corrugated by the grating, and n_c is the refractive index of the superstrate (air in this case), respectively. Note that the refraction of light on the boundary of the GC and the slab region is not considered here, because the angle change due to refraction is relatively small ($< 1°$) in our designs.

To use the tilted 1D GC for coupling light between a wire waveguide (with a width of 450 nm) and a single-mode fiber in free space, a long taper is normally needed between the waveguide and the GC. An FGC design can be used to dramatically reduce the length of this taper [11]. The curves of an FGC are described in a polar coordinate system as [3]

$$r(q, \alpha) = \frac{(q - q_0)\lambda_0}{n_g^0 - n_c \sin\phi_0 \cos(\alpha - \alpha_0)} + L(\alpha), \qquad (3)$$

where q_0 and $q \in N$ are the indices of the first and each line in the grating, respectively, and $L(\alpha)$ is the distance between the first line and the input waveguide (see fig. 1(b)). $L(\alpha)$ determines the waist size of the output light beam and has been discussed in detail in [3]. In the tilted FGCs, the azimuth α_0 is set different from 0° or 180°, in order to avoid the reflection fromIts variation going back to the input waveguide.

According to [9], [10], an extra Si overlay (polycrystalline or amorphous) with a thickness of 160 nm can be locally deposited on top of a 1D GC to increase the fraction of the upward diffracted power, so as to increase the waveguide-to-fiber coupling efficiency. The cross section of such a GC is shown in figure 2. In this letter, the 3D finite difference time domain (FDTD) method is used to analyze the power directionality of a tilted GC with a Si overlay. Considering the speed of the 3D FDTD simulations, the simulation domains (the dashed box in figure 2(a)) do not include the lower boundary of the 2 μm oxide layer. This is an acceptable approximation according to [9], which demonstrated that the influence of this boundary is less important for the GCs with Si overlays. This affirmation is also confirmed by a 2D FDTD simulation, which shows that the upward power of a GC with Si overlays is only increased by 0.7 dB (at 1550 nm) after considering this oxide layer. The widths of the input waveguide and the GC are set as 4 μm to further reduce the simulation time. For calculating the fraction of the upward diffracted power, this is a good approximation for the real case (10 μm width). However, this simplification can not be applied to tilted FGCs, which have more complex layouts. As a result, the simulations of tilted FGCs are more time and memory consuming compared to those of tilted 1D GCs.

The fractions of the upward coupled power ($\lambda_0 = 1550$ nm) of four groups of tilted 1D GC designs ($\phi_0 = 5°, 10°,$ 15° and 20°) with 160 nm Si overlays are simulated for
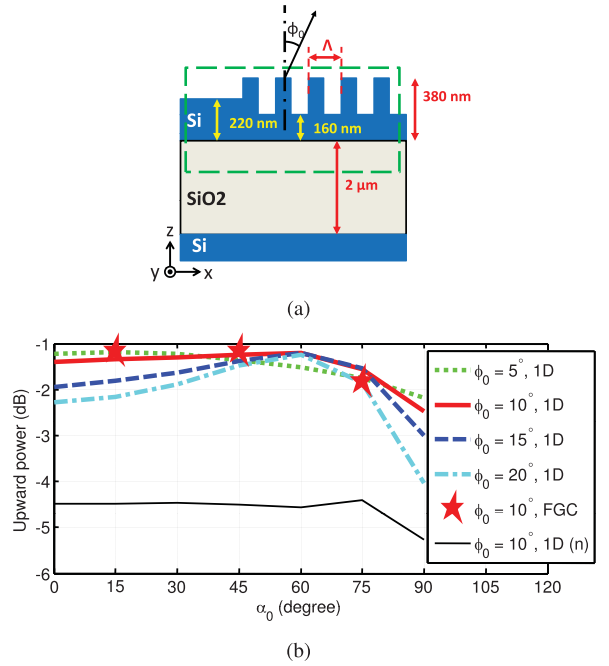

(a)

(b)

Fig. 2.   (a) The cross-section of a grating coupler with a silicon overlay; (b) fractions of light coupled into the upward direction of different tilted GCs as a function of the azimuth α_0 ($\lambda_0 = 1550$ nm). The curves called "1D" are for the tilted 1D GCs with a 160 nm thick Si overlay, the curves called "1D (n)" are for the tilted 1D GCs without Si overlay, and the curve called "FGC" is for a tilted FGC designed for $\alpha_0 = 15°, 45°, 75°$.

different α_0 values, and the results are illustrated in figure 2. In the simulations, n_g^0 is set to 2.75 to calculate the grating period and tilt angle according to eq. 1 and eq. 2, and $n_c = 1.0$, and the duty cycle of the gratings is set to 50% everywhere. It can be seen that the upward power of the tilted GC designs with $\phi_0 = 10°$ is always larger than -1.5 dB for $\alpha_0 \leq 60°$, and its variation is also smaller than that of the other tilted GCs. So the designs with $\phi_0 = 10°$ are chosen for further discussions in this letter. When $\alpha_0 \geq 75°$, the upward coupled power drops rapidly. This is because the period Λ is approaching the value that supports strong 2nd order reflections as α_0 is increasing. For comparison, the upward power coupling efficiency of tilted FGCs with the same Si overlay (designed for $\alpha_0 = 15°$, 45° and 75°) are also simulated and shown in figure 2(b). It is seen that the upward powers of the tilted FGC with Si overlay have similar values to those of the tilted 1D GCs with Si overlay designed with the same α_0 and ϕ_0. These results show that the upward power of tilted FGCs with Si overlay can be simply estimated from the results of tilted 1D GCs with Si overlay, which can be simulated more easily.

A group of tilted 1D GCs without the Si overlay (with 70 nm trench depth in the grating) are also simulated and shown in figure 2(b). Since the lower boundary of the oxide box is not considered in this simulation, the real upward powers for the normal tilted 1D GCs can be 1.5 dB greater (at 1550 nm) than these calculated values. But they are still less than those of the tilted 1D GCs with Si overlays.

Another important issue that can be found in figure 2(b) is that the tilted FGC designs can also enhance the coupling

efficiency. For example, the upward coupling efficiency for $\phi_0 = 20°$ is maximal when $\alpha_0 = 60°$, which is 1 dB stronger than the one with $\alpha_0 = 0°$. This is because, when $\phi_0 = 20°$, the thickness of the silicon overlay is not optimized for the design with $\alpha_0 = 0°$. Adjusting the thickness of the Si overly may optimize the transmission, but this is not practical due to fabrication limit, especially when two or more GCs designed for different zenith angles are simultaneously used in the same chip. In this case, the tilted design provides a different way to optimize the transmission.

One problem with this design is that n_g^0 can be wrongly estimated. Even if an accurate effective index value is obtained from simulation, the variation in this value caused by fabrication uncertainty is hardly controllable. As a result, the value of n_g^0 used in the design equations mentioned above is usually different from the real effective index of the grating. For clarification, a symbol n_g is used to stand for the index value used in the design, in order to be distinguished from the real index of the grating n_g^0. The difference between n_g and n_g^0 causes a direction change in the output light with the required wavelength and thus a central wavelength shift in the transmission spectrum. To find out the value of n_g^0 in real devices, one can make a scan of n_g and test the corresponding transmissions in measurement. However, scanning n_g is not a proper solution in many cases. Since the central wavelength shift is caused by the direction change of the output light with the required wavelength, there is a way to shift the central wavelength back to the required value by adjusting the direction of the output fiber to accommodate the new direction of the output light.

The new directions (α_0' and ϕ_0') can be theoretically calculated according to the following equations:

$$\alpha_0' = \alpha_0 + \arctan\left(\frac{\Delta n_g \sin\alpha_0}{n_{c,p} - \Delta n_g \cos\alpha_0}\right), \quad (4)$$

$$\phi_0' = \arcsin\left(\frac{\sqrt{n_{c,p}^2 + \Delta n_g^2 - 2n_{c,p}\Delta n_g \cos\alpha_0}}{n_c}\right), \quad (5)$$

where $\Delta n_g = n_g - n_g^0$. For $\alpha_0 = 45°$ and $\phi_0 = 10°$, the angle deviations $\Delta\alpha_0 = \alpha_0' - \alpha_0$ and $\Delta\phi_0 = \phi_0' - \phi_0$ are shown in figure 3. For both the tilted 1D GC and tilted FGC designs, these angle deviations can be used to adjust the output fiber direction.

The simulations of the reflection suppressions in tilted FGCs have already been reported in [12], and for tilted FGCs with Si overlay we have similar results. So they are not elaborated in this letter.

III. MEASUREMENT RESULTS AND DISCUSSIONS

A number of tilted focusing grating couplers with amorphous-Si overlays, designed for $\alpha_0 = 0°$ or $45°$, and $\phi_0 = 10°$, were fabricated through ePIXfab [13]. A scanning electron microscope image of a tilted FGC designed for $\alpha = 45°$ is shown in figure 4. Since different values of n_g were used in the place of n_g^0 in eq. 3 for different designs, these designs have different grating periods and shapes. As is
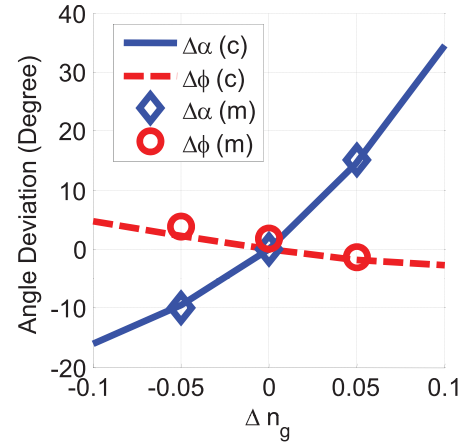

Fig. 3. The deviation of α_0 and ϕ_0 as a function of Δn_g. The solid and curved lines are calculated values. The $\Diamond$ and $\bigcirc$ symbols are the measured values.
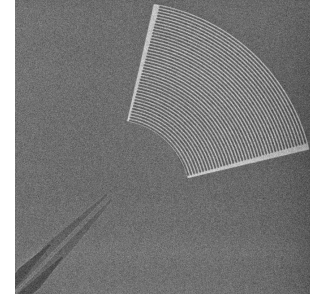

Fig. 4. A scanning electron microscope image of a tilted FGC designed for $\alpha = 45°$.

mentioned above, the azimuth of the out coupled light equals α_0. It is not possible to change the azimuths of the fibers in many measurement setups. In order to be used in these setups, the tilted FGCs and the input waveguides are purposely rotated around the surface normal with an angle of $-\alpha_0$ when they are designed on the PIC (see figure 4). The alignment procedure for these tilted FGCs is similar to that for a standard GC. For the tilted FGCs designed for $\alpha_0 = 45°$, the transmission spectra and the central wavelengths are changed corresponding to the different n_g values in the design (see figure 5). It can be seen that, for the tilted FGCs with silicon overlay, the waveguide-to-single mode fiber coupling losses are reduced by more than 2 dB compared to a standard grating coupler ("ref" in figure 5, without Si overlay, 70 nm etch depth, 625 nm period), and it is also 2 dB lower than that of the tilted FGCs without Si overlay ($\alpha_0 = 45°$, 70 nm etch depth) [3]. The lowest transmission loss is around -2.2 dB when $n_g = 2.75$, and this value is similar to that of a normal FGC with silicon overly ($\alpha_0 = 0°$) which is designed with the same n_g value. The central wavelength decreases linearly as n_g is increasing, with a slope of -0.4 μm per unit of index. The scanning results show that the real effective index n_g^0 at 1550 nm is about 2.65. As is mentioned above, the central wavelength shift for different n_g can be compensated by changing the fiber direction, which was observed in the measurements.
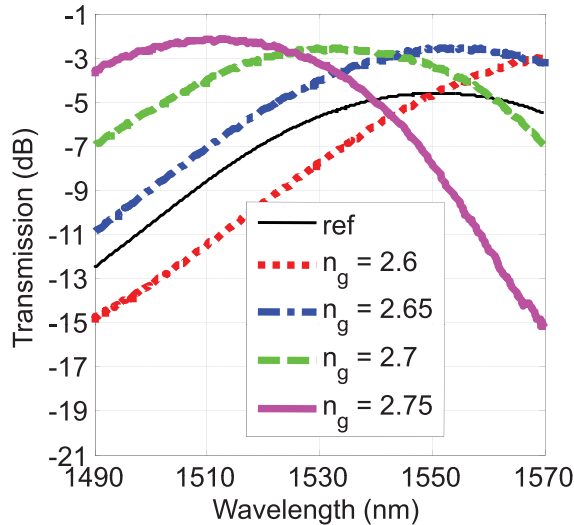
Fig. 5. Measured transmission spectra of four tilted FGCs with Si overlays with different n_g values, $\alpha_0 = 45°$. The "ref" curve stands for the transmission spectrum of a standard GC without any Si overlay.
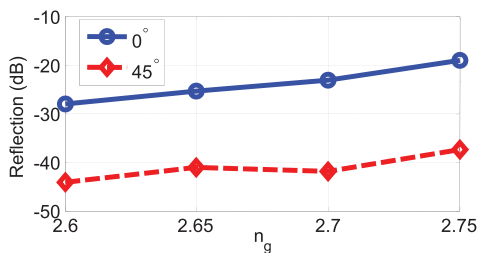

Fig. 6. The reflection values for FGCs with $\alpha_0 = 0°$ (solid line) and tilted FGCs with $\alpha_0 = 45°$ (dashed line). Both are with 160 nm thick Si overlay.

The measured deviations of the output light ($\Delta\alpha_0$ and $\Delta\phi_0$) are shown in figure 3. It is seen that the measured results agree well with the theoretically calculated ones.

The back reflections of tilted FGCs with $\alpha_0 = 0°$ and $45°$ are obtained by measuring the transmission fringes using an optical frequency domain reflectometry (OFDR) method. In order to split the reflections from the fiber end and those from the GCs, the end facets of both the input and output fibers are placed far away from the GCs. The results are shown in figure 6. It is found that, for $\alpha_0 = 0°$, the reflections are still considerably large (near -20 dB). For tilted FGCs with $\alpha_0 = 45°$, the reflection averaged in the frequency range from 1490 nm to 1570 nm can be reduced to lower than -40 dB. Note that these tilted FGCs with $\alpha_0 = 45°$ are the same tilted FGCs that yields the transmission spectra shown in figure 5.

IV. CONCLUSION

We reported the enhanced transmission in tilted one-dimensional grating couplers and tilted focusing grating couplers with the help of a locally deposited silicon overlay. Grating couplers with an enhanced waveguide-to-single mode fiber coupling efficiency (-2.2 dB) and a reduced back-reflection (around -40 dB) are realized with an advanced CMOS-compatible technology. Deviations in coupling wavelengths between design and experiment can be compensated by adjusting the directions of the output fiber.

REFERENCES

[1] D. Taillaert, et al., "An out-of-plane grating coupler for efficient butt-coupling between compact planar waveguides and single mode fibers," J. Quantum Electron., vol. 38, no. 7, pp. 949–956, 2002.

[2] D. Taillaert, P. Bienstman, and R. Baets, "Compact efficient broadband grating coupler for silicon-on-insulator waveguides," Opt. Lett., vol. 29, no. 23, pp. 2749–2751, 2004.

[3] Y. Li, D. Vermeulen, Y. De Koninck, G. Yurtsever, G. Roelkens, and R. Baets, "Compact grating couplers on silicon-on-insulator (SOI) with reduced back reflection," Opt. Lett., vol. 37, no. 21, pp. 4356–4358, 2012.

[4] C. Alonso-Ramos, A. Ortega-Monũx, I. Molina-Fernández, P. Cheben, L. Zavargo-Peche, and R. Halir, "Efficient fiber-to-chip grating coupler for micrometric SOI RIB waveguides," Opt. Express, vol. 18, no. 4, pp. 15189–15200, 2010.

[5] N. Na, et al., "Efficient broadband silicon-on-insulator grating coupler with low backreflection," Opt. Lett., vol. 36, no. 11, pp. 2101–2103, 2011.

[6] D. Wiesmann, "Apodized surface-corrugated gratings with varying duty cycles," IEEE Photon. Technol. Lett., vol. 12, no. 6, pp. 639–641, Jun. 2000.

[7] R. Halir, et al., "Continuously apodized fiber-to-chip surface grating coupler with refractive index engineered subwavelength structure," Opt. Lett., vol. 35, no. 19, pp. 3243–3245, 2010.

[8] Y. Tang, Z. Wang, L. Wosinski, U. Westergren, and S. He, "Highly efficient nonuniform grating coupler for silicon-on-insulator nanophotonic circuits," Opt. Lett., vol. 35, no. 8, pp. 1290–1292, 2010.

[9] G. Roelkens, D. V. Thourhout, and R. Baets, "High efficiency silicon-on-insulator grating coupler based on a poly-silicon overlay," Opt. Express, vol. 14, no. 24, pp. 11622–11630, 2006.

[10] D. Vermeulen, et al., "High-efficiency fiber-to-chip grating couplers realized using an advanced CMOS-compatible silicon-on-insulator platform," Opt. Express, vol. 18, no. 17, pp. 18278–18283, 2010.

[11] F. Van Laere, T. Claes, and J. Schrauwen, "Compact focusing grating couplers for silicon-on-insulator integrated circuits," IEEE Photon. Technol. Lett., vol. 19, no. 23, pp. 1919–1921, Dec. 1, 2007.

[12] D. Vermeulen, et al., "Reflectionless grating couplers for silicon-on-insulator photonic integrated circuits," Opt. Express, vol. 20, no. 20, pp. 22278–22283, 2012.

[13] (2013). ePIXfab, the Silicon Photonics Platform [Online]. Available: http://www.epixfab.eu